Lusi, a clastic-dominated geysering system in Indonesia recently explored by surface and subsurface observations

Karyono, Karyono; Obermann, Anne; Lupi, Matteo; Masturyono, Masturyono; Hadi, Soffian; Syafri, Ildrem; Abdurrokhim, Abdurrokhim; Mazzini, Adriano

How to cite

KARYONO, Karyono et al. Lusi, a clastic-dominated geysering system in Indonesia recently explored by surface and subsurface observations. In: Terra nova, 2017, vol. 29, n° 1, p. 13–19. doi: 10.1111/ter.12239

This publication URL: https://archive-ouverte.unige.ch/unige:95274
Publication DOI: 10.1111/ter.12239

Terra Nova

doi: 10.1111/ter.12239

Lusi, a clastic-dominated geysering system in Indonesia recently explored by surface and subsurface observations

Karyono Karyono,[1,2,3] Anne Obermann,[4] Matteo Lupi,[5] Masturyono Masturyono,[3] Soffian Hadi,[6] Ildrem Syafri,[2] Abdurrokhim Abdurrokhim[2] and Adriano Mazzini[1]

[1]*CEED, University of Oslo, Oslo, Norway;* [2]*Padjadjaran University (UNPAD), Bandung, Indonesia;* [3]*Agency for Meteorology, Climatology and Geophysics (BMKG), Jakarta, Indonesia;* [4]*Swiss Seismological Service, ETH Zurich, Zurich, Switzerland;* [5]*Department of Earth Sciences, University of Geneva, Switzerland* [6]*BPLS, Bandung, Indonesia*

ABSTRACT

The spectacular eruption of Lusi began in NE Java, Indonesia, on 29 May 2006 and is still ongoing. Since its birth, Lusi has presented a pulsating activity marked by frequent eruptions of gas, water, mud and clasts. The aim of this study was to bridge subsurface and surface observations to describe Lusi's behaviour. Based on visual observations from 2014 to 2015, Lusi's erupting activity is characterised by four recurrent phases: (1) regular bubbling activity; (2) clastic geysering; (3) clastic geysering with mud bursts and intense vapour discharge; (4) quiescent phase. With a temporary network of five seismic stations deployed around the crater, we could identify tremor events related to phases 2 and 3. One of the tremor types shows periodic overtones that we associate with mud wagging in the feeder conduit. On the basis of our observations, we would describe Lusi as a sedimentary-hosted hydrothermal system with clastic-dominated geysering activity.

Terra Nova, 29: 13–19, 2017

Introduction

On 29 May 2006, numerous SW–NE aligned sites, erupting hot mud, appeared in NE Java in the Sidoarjo district (Fig. 1A). Within weeks, a prominent eruption site, named Lusi, flooded a surface of nearly 1.5 km^2. The mud-flooded area became gradually larger in size. Today, a 10 m high embankment frames a region of 7 km^2 to protect the surrounding settlements and prevent Lusi from flooding the region any further. Currently, Lusi is still active and, to our knowledge, is the largest ongoing and most destructive mud-erupting system on Earth.

Since the early stages, Lusi has shown high temperatures (i.e. a temperature gradient of 42 °C km^{-1}, with crater temperatures of ~100°C) and a pulsating behaviour with powerful mud and vapour bursts occurring with a changing periodicity (e.g. around 30 min in September 2006, 1.5 h in June 2007, and 15 min now). These observations, combined with fluid analyses, led Mazzini *et al.* (2007) to propose the concept of a 'quasi hydrothermal system'. Further geochemical analyses of the erupted fluids (98% water, 1.5% CO_2, 0.5% CH_4; Mazzini *et al.*, 2012; Vanderkluysen *et al.*, 2014) confirmed the hydrothermal signature and high temperature reactions. Mazzini *et al.* (2012) described Lusi as a newborn *sedimentary-hosted hydrothermal system* (SHHS) with pulsating activity fed by magmatic fluids migrating from the neighbouring Arjuno–Welirang volcanic complex (Fig. 1B). This definition provided a distinct classification of the Lusi phenomenon, which differs from a mud volcano. Converging definitions and characteristics from various authors define mud volcanism, or *sedimentary volcanism*, as typically methane-dominated. The initiation of such volcanism is commonly driven by gravitative instability; it occurs in 'cold' sedimentary basins and is typically related to the presence of natural hydrocarbon reservoirs, with eruptions usually lasting hours or up to some days (e.g. Milkov, 2000; Dimitrov, 2002; Kopf, 2002; Revil, 2002; Abrams, 2005; Etiope, 2015). While some authors still include in the definition of sedimentary volcanism manifestations connected with hydrothermal activity, others (since the 1960s) stress the fact that SHHS are substantially different. In fact, these hybrid systems result from magmatic or hydrothermal CO_2-rich and vapour-rich fluids, related to igneous intrusions and high temperature geothermal fluids, crossing or interacting with organic-rich and CH_4-rich sedimentary rocks, resulting in the production of complex high temperature gas mixtures of different origins. Lusi has the same characteristics as other known SHHS hybrid systems described from other localities worldwide (e.g. Helgeson, 1968; Von Damm *et al.*, 1985; Welhan and Lupton, 1987; Simoneit, 1988, Jamtveit *et al.*, 2004; Svensen *et al.*, 2004, 2009; Zarate-del Valle and Simoneit, 2005; Mazzini *et al.*, 2011, 2014; Ciotoli *et al.*, 2016).

Since its birth, Lusi has exhibited long-term flow rate fluctuations as well as short-term (i.e. approximately every 30 min) events of enhanced activity. In this study, we test the proposed SHHS scenario by investigating and documenting the short-term events monitored during field campaigns in 2014 and 2015 and collecting surface and subsurface observations. We argue that Lusi can be described as a (so far undocumented) clastic-dominated geysering system.

Correspondence: Dr. Anne Obermann, SED, ETH, Sonneggstrasse 5, Zürich 8006, Switzerland. E-mail: anne.obermann@sed.ethz.ch

Methods

Seismic stations in the embankment area

To monitor Lusi's activity, we deployed five seismic stations inside Lusi's embankment from 4 to 10

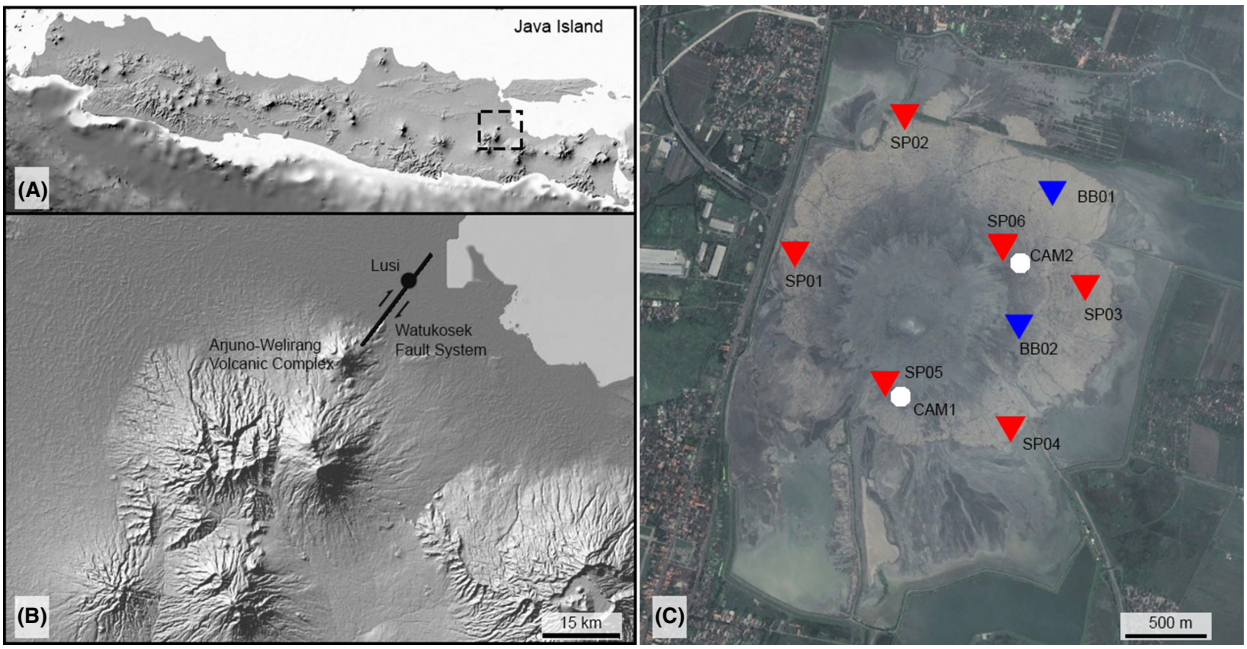

Fig. 1 (A) Map of Java. (B) Elevation map of Eastern Java, with the volcanic arc and back arc basin in the north-east of the island. Lusi and other mud volcanoes are located along the Watukosek fault system (black line). (C) Aerial view of the Lusi mud volcano showing the positions of the short-period stations SP01–SP04 and the broadband station BB01 deployed during the 5-day field experiment (inverted triangles), as well as the positions of the cameras (Cam1, Cam2, white circles) and the associated short-period stations SP05, SP06 and the broadband station BB02 (inverted triangles) within the embankment area. [Colour figure can be viewed at wileyonlinelibrary.com].

November 2014 (Fig. 1C). We used one broadband (Trilium 120s compact, BB01 Nanometrics, Calgary, Canada) and four short-period sensors (Leinartz 3Dlite, SP01-SP04 Lennartz electronics GmbH, Tübingen, Germany) equipped with Taurus digitizers. The sampling rate was set to 100 Hz. The sensors were buried at approximately 1 m depth, thermally insulated and covered with sediments (i.e. clays) to improve the signal-to-noise ratio and were deployed on a concrete plate. All sensors were located between 400 and 1200 m from the eruption centre. In a second experiment on 11 June 2015, a short-period sensor (SP05) was placed at the edge of the crater, in the southern part. The experiment was replicated between 9 and 11 November, with two sensors (BB01, SP06) deployed at the north-eastern edge of the crater. The three experiments revealed the same type of waveforms, showing the consistency of our findings.

Visual observations

During the second experiment and its replication, the seismic recording was coupled with an HD camera positioned in the embankment (Fig. 1C), with the purpose of continuously recording Lusi's eruptive behaviour and linking it to the seismic activity. The camera recorded 3 h of crater activity on 11 June, and 18.50 hours on 9–11 November 2015. The images were analysed and the eruptive phases classified. The video camera time record was synchronised with the logging of the seismometer with a synchronisation error as large as 1 s.

Results

Visual observations: eruption cycles

On the basis of visual observations and HD camera records, we identify four phases characterising Lusi's activity.

1 *Regular bubbling activity* (Fig. 2A): This phase consists of the constant emission of mud breccia (i.e. viscous mud containing clay, silt, sand and clasts of up to 10 cm in diameter) associated with the expulsion of water in both a liquid and a vapour state as well as of other gasses (Mazzini *et al.,* 2012; Vanderkluysen *et al.,* 2014). The typical duration of this phase is around 5 min, but it has been observed to last up to 10 min.
2 *Enhanced bubbling and mud bursts* (Fig. 2B): This interval consists of limited vapour emissions and vigorous mud bursting activity at the crater site. This phase typically begins with decimetre-sized bubbles that appear scattered throughout the crater zone. Within a few seconds, the bubbles increase in size, reaching up to 5–10 m in diameter and height. This phase is typically short-lived, with a duration of around 30 s.
3 *Enhanced bubbling with intense vapour* (Fig. 2C): This interval is characterised by a noisy and vigorous degassing discharge and a dense plume that may rise up to 100 m above the ground. Occasional strong winds may disperse the plume and reveal that, during this phase, large bursts (i.e. like in phase 2) still occur inside the crater. During this phase there is a significant increase in the water level of the streams that radially flush the mud from the crater. This

indicates that an increased amount of water is also discharged during this phase. The duration may vary between 2 and 10 min.

4 *Quiescent phase* (Fig. 2D): This interval marks the end of the venting activity during which no gas emissions or bursts are observed. During this phase, the system reaches an almost complete halt that may last from 1 to 2 min.

In Fig. 3, we show two 3 h eruptive cycles, observed on 11 June 2015 (A) and 11 November 2015 (B), that show snapshots of Lusi's eruptive behaviour. Each phase has a distinct colour and is plotted at a different height to facilitate reading. The interval durations are not uniformly distributed and may vary from one cycle to another. Only about 50% of the cycles include all of the four described phases. On average, two cycles occur every 30 min. In November 2015 (Fig. 3B), the length of phases 2 and 3 increased. Overall, throughout the observation period, the regular phase 1 activity is more frequent, but variations may occur in the other phases depending on the monitoring period. The time intervals between the phases could be subject to change. Due to a lack of systematic observation, we can only hypothesise that dry and wet seasons have an influence here.

Characterisation of seismicity at Lusi

We analysed the records from the seismic stations during the 1-week recording and identified two types of seismic signals beneath Lusi:

1 Microseismic events: These events are characterised by a sharp onset of the P-waves with clear S-wave arrivals (Fig. 4A, upper part). The frequency band for these seismic events ranges from 5 to 25 Hz (Fig. 4A, lower part). The signal duration is about 20 s. During the 1-week deployment, we observed three microseismic events with magnitudes around MI 1.7 ± 0.1 that were clearly identified by all 5 seismic stations and that were also picked up by some of the regional permanent stations that are operated by the BKGM. The epicentres fell inside the embankment.

2 Tremor events: These can be divided into two categories:

i *The tremor type-1* events have dominant frequencies ranging from 5 to 10 Hz (Fig. 4B, lower part) with an emergent behaviour. From the signal envelopes (Fig. 5A) we identified a typical tremor duration of 20–30 s. During the 1-week recording, we identified a total of 154 tremor type-1 events at at least three stations.

ii *The tremor type-2* events are roughly three times more powerful than the tremor type-1 events (Fig. 5). We observed 7–8 equally spaced overtones that are visible from 2 to 15 Hz (Fig. 4C). The overtones are

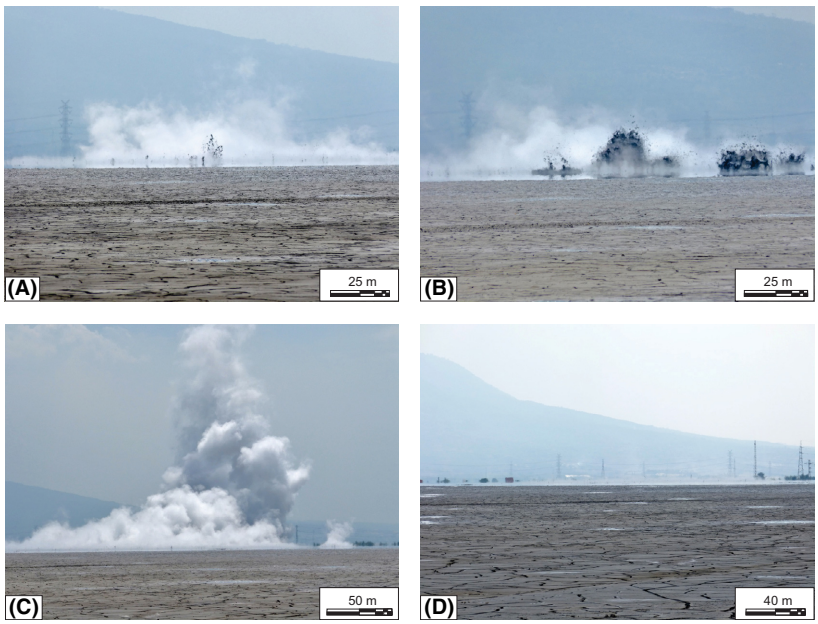

Fig. 2 Four phases of the eruptive cycles at the Lusi eruption site: (A) regular bubbling activity, (B) clastic geysering, (C) clastic geysering with intense vapour, and (D) quiescent phase where no activity is observed. [Colour figure can be viewed at wileyonlinelibrary.com].

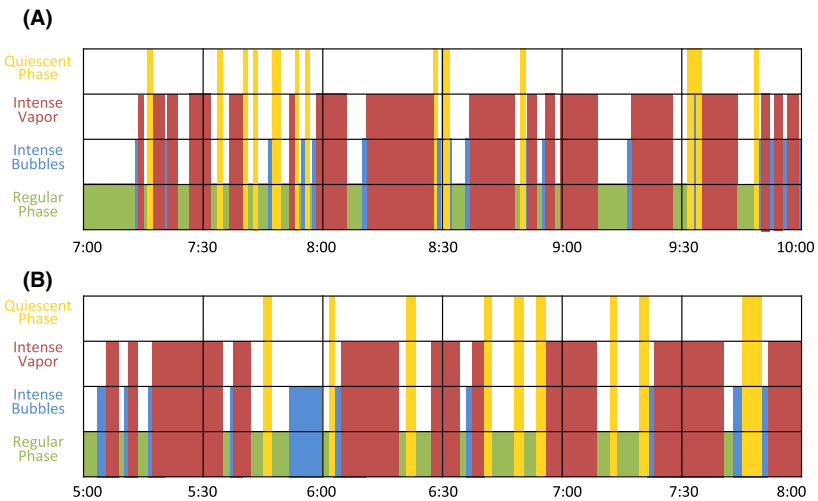

Fig. 3 Three hours of eruptive cycles at the Lusi mud volcano on (A) 11 June 2015 and (B) 11 November 2015. The different colours and column heights represent the four different cycle phases: regular phase (green), intense bubbles (blue), intense vapour (red) and quiescent phase (yellow). [Colour figure can be viewed at wileyonlinelibrary.com].

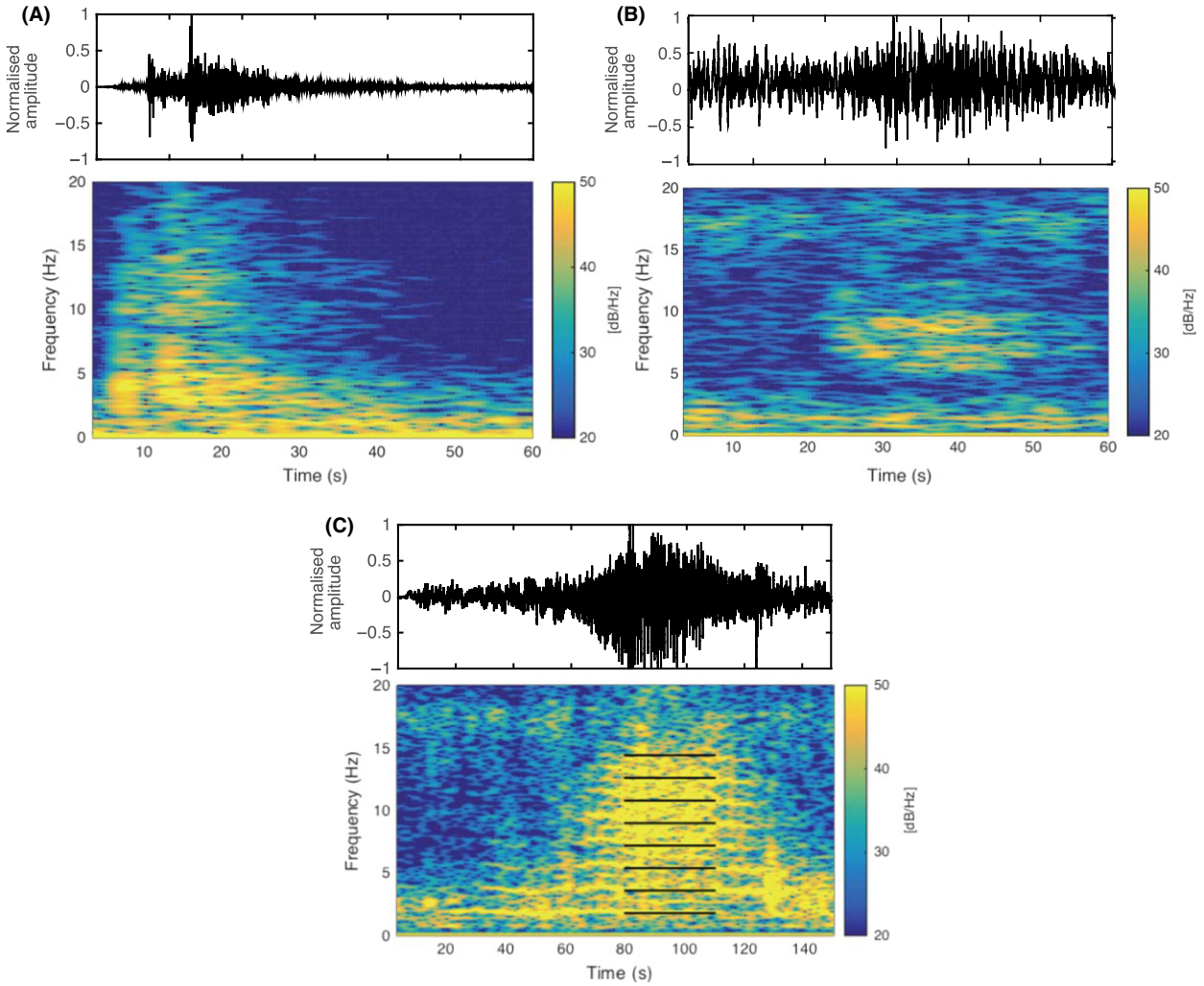

Fig. 4 Exemplary waveforms and spectrograms of the different types of seismic events that we find at the Lusi mud volcano: (A) microseismic event (SP02), (B) tremor type-1 with dominant frequencies between 5 and 10 Hz, lasting for about 30 s (SP01), and (C) long-lasting tremor type-2, exciting frequency bands from 5 to 15 Hz with clear harmonic overtones (SP06). [Colour figure can be viewed at wileyonlinelibrary.com].

narrow-banded at the beginning and end of the tremor, whereas they become 'broadband' coincident with the highest signal amplitude. No difference in amplitude between the fundamental frequency and the higher harmonics is observed. This tremor type typically lasts from 80 s to 180 s (Fig. 5B). During the 1-week recordings, we identified a total of 34 tremor type-2 events at at least three stations.

On the spectrograms of the stations in the direct vicinity of the crater (SP05, SP06), we observed a continuous excitation of the 15–20 Hz frequency band (Fig. 4B,C). This excitation is absent for the stations located further away from the crater edge (e.g. Fig. 4A).

In general, we notice a remarkable difference in the signal-to-noise ratio in the stations near the crater compared with the ones located further away. This could be due to the strong attenuation effect of the clay filling the embankment around Lusi, which may dampen the noise generated by the upwelling fluids in the crater. This is supported by the delay of the first arrivals of P-waves at some seismic stations. The station closest to the crater is SP04 (about 700 m away from the eruptive crater), while the most distant is SP02 (at about 1200 m). The delay of P-wave arrivals at SP02 is about 2 s compared with the arrival of P-waves at SP04. This implies a strong attenuation of the seismic signal over a very short distance (i.e. 500 m).

Relation between seismic and eruptive activity

To investigate whether the observed tremors are related to the eruption activity, we coupled the HD camera and seismic records. We observed that 90% of the tremor events were associated with the enhanced phases 2 and 3. The onset of such signals precedes the visual evidence of enhanced activity phases at the surface by typically 3 (±1) s.

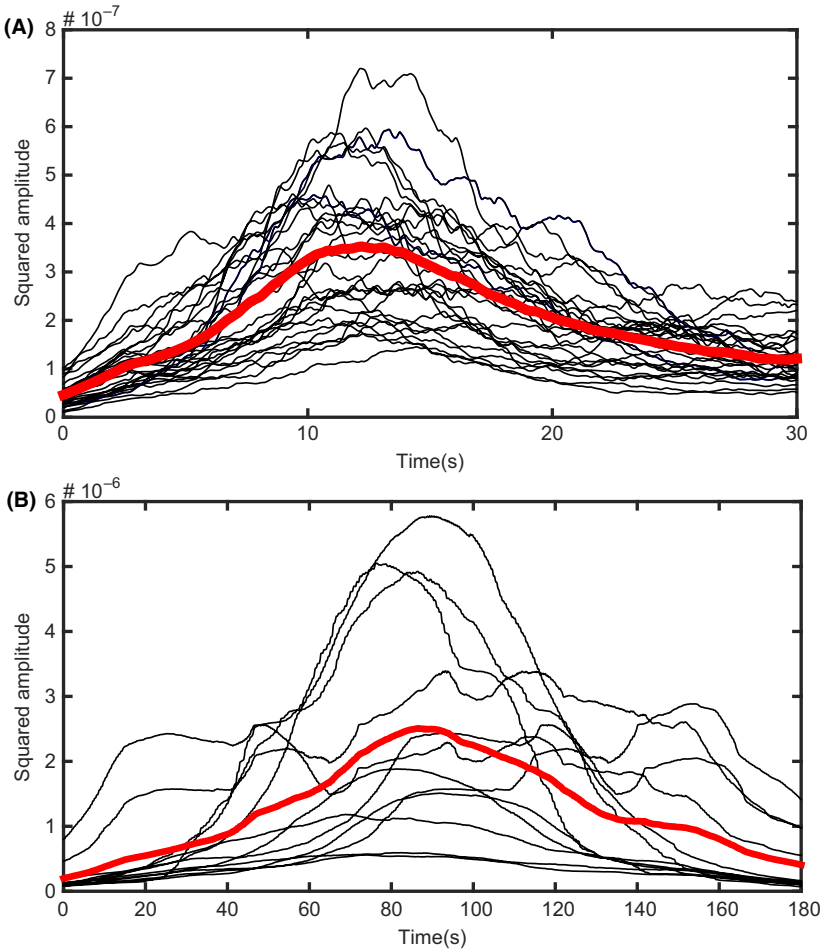

Fig. 5 Amplitude envelopes of the two tremor types, as recorded on SP01. The thick red line is the average envelope. (A) Thirty-seven tremor type-1 events typically lasting about 30 s. (B) Twelve tremor type-2 events lasting for 80–180 s. [Colour figure can be viewed at wileyonlinelibrary.com].

Discussion

Dynamics at the crater site

Both tremor types appear to be connected to the erupting behaviour of Lusi, and most specifically to phases 2 and 3 (enhanced bubbling with mud bursts and intense vapour). The features of tremor type-1 resemble degassing events on volcanoes (Ripepe *et al.*, 2010). Tremor type-2 shows very distinct, regularly spaced overtones, as observed in harmonic tremors. This tremor could be related to mud wagging in the feeder conduit while the gas bubbles ascend (Bercovici *et al.*, 2013).

In general, we do not always observe the tremors at all five stations positioned around the crater edge, suggesting that the attenuation could be related to a very shallow origin of the signal. Considering the consistent delay of 3 ± 1 s between the signal recorded by the seismic stations and the visual observation of the eruption, we use a simple geometric calculation (see Appendix S1) to roughly approximate the signal origin depth as ~30 m. Although we use a different approach, this depth estimate coincides with the one calculated by Vanderkluysen *et al.*, 2014, which they suggested was the depth at which decompressional boiling occurs.

Lusi and geysering activity

The vigour and the periodicity of the venting phases observed at Lusi resemble those of water-dominated geysers observed in other settings (e.g. Kedar, 1996). For this reason, for Lusi, we propose calling the phases 'enhanced bubbling and mud bursts' (Fig. 2B) and 'enhanced bubbling with intense vapour' (Fig. 2C) 'clastic geysering' and 'clastic geysering with intense vapour', respectively (see video in the online supplemental material). In general, two physical models have been proposed (and adjusted through time) to explain the mechanisms governing traditional geysering activity. Mackenzie (1811) suggests a contorted plumbing system with a large cavity where rising bubbles build an overpressure of steam that is periodically released through pipes. The alternative and most broadly diffused model suggests a vertical conduit with sudden flashing of superheated water into steam when hydrostatic pressure drops (Bunsen, 1847).

We believe that neither of the two models described above is *per se* applicable at Lusi. First, Lusi is clastic-dominated and, unlike the water-dominated geysers that commonly occur in cemented rocks, shows different rheologies and reactions occurring in its conduit. Second, Lusi's plumbing system might be much more complicated as the eruption site sits upon a fault system (i.e. Watukosek fault system) (Mazzini *et al.*, 2009).

We therefore suggest a preliminary model that explains the observations and the collected seismic data. High temperature fluids are vented in the Lusi conduit, rising from high- to low-pressure levels. As the fluids ascend towards the shallow subsurface, they approach the water vapour region and the sudden pressure drop triggers flashing and the exsolution of the dissolved CO_2 and CH_4 following a model similar to that described by Mazzini *et al.* (2012) and Vanderkluysen *et al.* (2014). The periodicity of the four described phases (Fig. 3) is not precisely regular. We suggest that this irregularity could be related to the random and semi-continuous discharge of water and clastic material, which slightly alters the morphology at the crater site after each geysering event. Therefore, the pressure decrease required to initiate fluids flashing (i.e. the volume of water and mud that must be removed from the crater site to cause

the hydrostatic pressure drop) does not occur systematically (e.g. unlike as described in Ingebritsen and Rojstaczer, 1993).

The presence of vigorous bubbling activity during phase 2 and the absence of an aqueous vapour plume being expelled suggest that significant amounts of gas are being released during this phase. The most likely candidates to propel this type of activity are CO_2 and CH_4. We propose that during the initial geysering phase, these two gasses move faster towards the surface, producing these large bubbles. The aqueous vapour reaches the surface later, interacting with additional CO_2 and CH_4, and then initiates phase 3.

Geochemistry shows that Lusi fluids migrate from great depth through several sedimentary formations (Mazzini *et al.*, 2012). We suggest that the rise of deep fluids into the more deformable Kalibeng Fm. at around 1–1.5 km triggers inflation/deflation inside this easily eroded package, therefore contributing to a periodic charge and discharge of the system. Fluids then upwell along the fractured zone below Lusi (Mazzini *et al.*, 2009) to trigger the geysering activity described above.

The presence of periodic geysering behaviour at Lusi is consistent with the activity of an erupting hybrid phenomenon such as an SHHS. These results strengthen the hypothesis that, in the Lusi region, all the ingredients necessary to trigger sedimentary volcanism phenomena are present and that this process was accelerated, enhanced and chemically altered by the activity of the connected Arjuno–Welirang magmatic complex. The final result was the most spectacular clastic-dominated erupting geyser on Earth.

Conclusions

The results reported herein are the first detailed description of the erupting activity observed at Lusi during three field campaigns. We coupled visual observation with seismic records, showing that Lusi's behaviour is characterised by four phases that replicate in cyclical order in time. The documented activity of Lusi can be summarised as: (1) regular bubbling activity, (2) clastic geysering, (3) clastic geysering with intense vapour and (4) quiescent phase.

With the seismic stations, we recorded microseismic and two distinct types of tremor within Lusi's embankment. The tremor events are associated with Lusi's activity phases 2 and 3. Of particular interest is the tremor type-2, which shows harmonic overtones that resemble harmonic tremors due to magma wagging in volcanoes.

We propose a mechanism fuelling Lusi geysering activity that occurs at relatively shallow depths. In our proposed model, deep hot hydrothermal fluids upwell along the faulted and brecciated geological units. The deep fluids reach an accumulation reservoir located in the Kalibeng Fm. (~1–1.5 km), which inflates and deflates according to the flow rate reaching the reservoir. The hot fluids are then vented to the surface along a conduit promoting flashing and exsolution reactions, releasing CO_2, CH_4 and aqueous vapour. When the deep fluid mixture phase separates, the coalescing, imploding and exploding bubbles initiate the geysering activity.

Our multidisciplinary approach is an effort to understand the mechanism controlling this new geological phenomenon. To our knowledge, Lusi is the first documented example of a sedimentary-hosted hydrothermal system with clastic-dominated geysering activity.

Acknowledgements

The research leading to these results was funded by the European Research Council under the European Union's Seventh Framework Programme Grant agreement no. 308126 (LUSI LAB project). The Research Council of Norway, through its Centres of Excellence funding scheme (project number 223272), is thanked for support during this work. We thank the Geophysical Instrument Pool Potsdam (GIPP) for providing the instruments for the SEED experiments in the framework of the LUSI LAB project. Anne Obermann (EUSFP, Project IMAGE grant no. 608553) and Matteo Lupi (SNF Ambizione grant no. PZ00P2_154815) are also part of the SCCER collaborative environment. We thank the Associate Editor Ghislain de Marsily, Dr Mark Tingay and an anonymous reviewer for their precious help and suggestions that improved this manuscript.

References

Abrams, M.A., 2005. Significance of hydrocarbon seepage relative to petroleum generation and entrapment. *Mar. Pet. Geol.*, **22**, 457–477.

Bercovici, D., Jellinek, A.M., Michaut, C., Roman, D.C. and Morse, R., 2013. Volcanic tremors and magma wagging: gas flux interactions and forcing mechanism. *Geophys. J. Int.*, **195**, 1001–1022.

Bunsen, R.W., 1847. Physikalische Beobachtungen uber die hauptsachlichsten Geysir Islands. *Ann. Phys. Chemie*, **83**, 159–170.

Ciotoli, G., Etiope, G., Marra, F., Florindo, F., Giraudi, C. and Ruggiero, L., 2016. Tiber delta CO2-CH4 degassing: a possible hybrid, tectonically active Sediment-Hosted Geothermal System near Rome. *J. Geophys. Res. Solid Earth*, **1**, 48–69. doi:10.1002/2015JB012557.

Dimitrov, L.I., 2002. Mud volcanoes–the most important pathway for degassing deeply buried sediments. *Earth Sci. Rev.*, **59**, 49–76.

Etiope, G., 2015, *Natural Gas Seepage. The Earth's Hydrocarbon Degassing*. Springer International Publishing Switzerland, ISBN 978-3-319-14601-0 (eBook), DOI 10.1007/978-3-319-14601-0, 199 pp.

Helgeson, H.C., 1968. Geologic and thermodynamic characteristics of Salton Sea geothermal system. *Am. J. Sci.*, **266**, 129–166.

Ingebritsen, S.E. and Rojstaczer, S.A., 1993. Controls on geyser periodicity. *Science*, **262**, 889–889.

Jamtveit, B., Svensen, H., Podladchikov, Y. and Planke, S., 2004. Hydrothermal vent complexes associated with sill intrusions in sedimentary basins. *Geol. Soc. London Spec. Publ.*, **234**, 233–241.

Kedar, S., 1996. The origin of harmonic tremor at Old Faithful geyser (Doctoral dissertation, California Institute of Technology).

Kopf, A.J., 2002. Significance of mud volcanism. *Rev. Geophys.*, **40**(2), 1–52.

Mackenzie, G.S., 1811. *Travels in the Island of Iceland*. Edinburgh, Allam and Company. 27 p.

Mazzini, A., Svensen, H., Akhmanov, G.G., Aloisi, G., Planke, S., Malthe-Sorenssen, A. and Istadi, B., 2007. Triggering and dynamic evolution of the LUSI mud volcano, Indonesia. *Earth Planet. Sci. Lett.*, **261**(3–4), 375–388.

Mazzini, A., Nermoen, A., Krotkiewski, M., Podladchikov, Y., Planke, S. and Svensen, H., 2009. Strike-slip faulting as a trigger mechanism for overpressure release through piercement structures. Implications for the Lusi mud volcano,

Indonesia. *Mar. Pet. Geol.*, **26**(9), 1751–1765.
Mazzini, A., Svensen, H., Etiope, G., Onderdonk, N. and Banks, D., 2011. Fluid origin, gas fluxes and plumbing system in the sediment-hosted Salton Sea Geothermal System (California, USA). *J. Volcanol. Geoth. Res.*, **205**, 67–83.
Mazzini, A., Etiope, G. and Svensen, H., 2012. A new hydrothermal scenario for the 2006 Lusi eruption, Indonesia. Insights from gas geochemistry. *Earth Planet. Sci. Lett.*, **317**, 305–318.
Mazzini, A., Hadi, S., Etiope, G. and Inguaggiato, S., 2014, Tectonic Control of Piercement Structures in Central Java, Indonesia. American Geophysical Union, Fall Meeting 2014, abstract #OS21B-1138, v. #OS21B-1138
Milkov, A.V., 2000. Worldwide distribution of submarine mud volcanoes and associated gas hydrates. *Mar. Geol.*, **167**, 29–42.
Revil, A., 2002. Genesis of mud volcanoes in sedimentary basins: a solitary wave-based mechanism. *Geophys. Res. Lett.*, **29**(12), 1–4. doi:10.1029/2001GL014465.
Ripepe, M., Marchetti, E., Bonadonna, C., Harris, A.J., Pioli, L. and Ulivieri, G., 2010. Monochromatic infrasonic tremor driven by persistent degassing and convection at Villarrica Volcano, Chile. *Geophys. Res. Lett.*, **37**(15), 1–6.
Simoneit, B.R.T., 1988. Petroleum generation in submarine hydrothermal systems - an update. *Can. Mineral.*, **26**, 827–840.
Svensen, H., Planke, S., Malthe-Sørenssen, A., Jamtveit, B., Myklebust, R., Eidem, T. and Rey, S.S., 2004. Release of methane from a volcanic basin as a mechanism for initial Eocene global warming. *Nature*, **429**, 542–545.
Svensen, H., Hammer, Ø., Mazzini, A., Onderdonk, N., Polteau, S., Planke, S. and Podladchikov, Y.Y., 2009. Dynamics of hydrothermal seeps from the Salton Sea geothermal system (California, USA) constrained by temperature monitoring and time series analysis. *J. Geophys. Res. Solid Earth*, **114**, B09201.
Vanderkluysen, L., Burton, M.R., Clarke, A.B., Hartnett, H.E. and Smekens, J.F., 2014. Composition and flux of explosive gas release at LUSI mud volcano (East Java, Indonesia). *Geochem. Geophys. Geosyst.*, **15**(7), 2932–2946.
Von Damm, K.L., Edmond, J.M., Measures, C.I. and Grant, B., 1985. Chemistry of submarine hydrothermal solutions at Guaymas Basin, Gulf of California. *Geochim. Cosmochim. Acta*, **49**, 2221–2237.
Welhan, J.A. and Lupton, J.E., 1987. Light-hydrocarbon gases in Guaymas Basin hydrothermal fluids - thermogenic versus abiogenic origin. *Bull. Am. Assoc. Petrol. Geol.*, **71**, 215–223.
Zarate-del Valle, P.F. and Simoneit, B.R.T., 2005. Hydrothermal bitumen generated from sedimentary organic matter of rift lakes - Lake Chapala, Citala Rift, western Mexico. *Appl. Geochem.*, **20**, 2343–2350.

Received 24 March 2016; revised version accepted 23 September 2016

Supporting Information

Additional Supporting Information may be found in the online version of this article:

Appendix S1. Calculation for depth of bubble release.

Video S1. 4 phases of Lusi.

